Research Square

Preprints are preliminary reports that have not undergone peer review.
They should not be considered conclusive, used to inform clinical practice,
or referenced by the media as validated information.

Nested and Additive Skew-Gaussian Tukey-h Processes for Environmental Extremes

Negar Alizadeh
Tarbiat Modares University
Majid Jafari Khaledi
jafri-m@modares.ac.ir
Tarbiat Modares University
Hamid Zareifard
Jahrom University

Research Article

Keywords: Geostatistics, Skew-normal tukey-h distribution, Heavy tails, Skewness, Bayesian hierarchical models, Spatial Random effects

Posted Date: May 8th, 2026

DOI: https://doi.org/10.21203/rs.3.rs-9385614/v1

License: This work is licensed under a Creative Commons Attribution 4.0 International License.
Read Full License

Additional Declarations: No competing interests reported.

Nested and Additive Skew-Gaussian Tukey-*h* Processes for Environmental Extremes

Negar Alizadeh[a], Majid Jafari Khaledi[a,*] and Hamid Zareifard[b]

[a]*Department of Statistics, Tarbiat Modares University, P.O. Box 14115-134, Tehran, Iran*
[b]*Department of Statistics, Jahrom University, Jahrom 74137-66171, Iran*

ARTICLE INFO

Keywords:
Geostatistics
Skew-normal tukey-*h* distribution
Heavy tails
Skewness
Bayesian hierarchical models
Spatial Random effects

ABSTRACT

Spatial data arising in environmental and ecological studies often exhibit marked skewness and heavy-tailed behavior, posing challenges for conventional Gaussian spatial random effects models. To address these limitations, we develop a class of skew-Gaussian Tukey-*h* (SGTH) spatial processes that provide flexible control over both skewness and tail heaviness. We introduce two constructions of SGTH spatial fields, referred to as the nested and additive formulations, which induce non-Gaussian behavior through distinct structural mechanisms. We investigate key marginal and dependence properties of the proposed processes and embed them within a Bayesian hierarchical framework for modeling spatially indexed data using SGTH random effects. Posterior inference is conducted via Markov chain Monte Carlo methods, using a data augmentation strategy and scalable local updates to handle the non-Gaussian latent structure. Through simulation studies, we explore the inferential behavior of the two constructions and illustrate their practical implications. The proposed methodology is further demonstrated through the analysis of a georeferenced rainfall dataset.

1. Introduction

Gaussian processes serve as the cornerstone of classical geostatistical modeling, largely due to their mathematical tractability and well-established inferential framework. Despite their widespread application, Gaussian-based models are inherently limited in capturing essential features often found in environmental and ecological data, such as pronounced skewness and heavy-tailed behavior (see, e.g., Zhang et al. (2024)). Such departures from normality are frequently observed in variables like precipitation and temperature extremes; ignoring these characteristics can lead to biased inference and substantially degraded predictive performance.

To accommodate asymmetry in spatial data, skew-Gaussian random fields have been proposed as flexible extensions of Gaussian processes. In particular, constructions based on the skew-normal distribution (Azzalini, 1985) allow for controlled skewness while retaining analytical tractability and including the Gaussian model as a special case (Zhang and El-Shaarawi, 2010). However, the skew-normal distribution is characterized by bounded kurtosis (Azzalini and Capitanio, 2014), which limits its ability to represent heavy-tailed behavior and extreme spatial events commonly encountered in environmental applications.

Several methodological developments have been introduced to overcome these limitations, including trans-Gaussian approaches such as Tukey *g*-and-*h* random fields (Xu and Genton, 2017), skew-Gaussian scale mixtures (Zareifard and Khaledi, 2013), and spatial skew-*t* processes (Bevilacqua et al., 2021). While these models substantially enhance flexibility, they often entail substantial computational challenges, particularly in Bayesian settings where non-Gaussian latent structures lead to complex posterior distributions and poor mixing of standard MCMC algorithms. As a result, achieving a balance between distributional flexibility, interpretability, and computational scalability remains an open problem in non-Gaussian spatial modeling.

In this paper, we develop a class of skew-Gaussian Tukey-*h* (SGTH) spatial fields designed to flexibly capture both skewness and tail heaviness. We introduce two complementary constructions. The first, referred to as the nested SGTH spatial field, is obtained by applying the Tukey-*h* transformation to a skew-Gaussian process, extending the skew-normal Tukey-*h* distribution (Mondal and Genton, 2024) to a spatial setting. This construction provides a useful theoretical benchmark with analytically tractable dependence properties. The second, termed the additive SGTH spatial

*Corresponding author
jafari-m@modares.ac.ir (M. Jafari Khaledi); zareifard@jahromu.ac.ir (H. Zareifard)

field, employs an alternative structure in which skewness and tail behavior are induced through separate components. This decoupling leads to improved identifiability and more stable posterior inference in practice.

We investigate the distributional properties of both constructions and embed them within a Bayesian hierarchical framework for spatial modeling. Posterior inference is performed using Markov chain Monte Carlo methods, leveraging data augmentation and computationally efficient local updates to handle the non-Gaussian latent structure. The practical behavior of the models is examined through simulation studies, and an application to georeferenced rainfall data illustrates the utility of the proposed approach.

The remainder of the paper is organized as follows. Section 2 introduces the SGTH spatial field constructions and their distributional properties. Section 3 presents the Bayesian modeling framework and posterior computation. Section 4 reports simulation studies comparing the two constructions. Section 5 provides an application to rainfall data, and Section 6 concludes with discussion and directions for future research.

2. Two Constructions for Skew-Gaussian Tukey-h Spatial Fields

This section introduces two alternative constructions for defining Skew-Gaussian Tukey-h (SGTH) spatial random fields. Both constructions are designed to jointly accommodate skewness and heavy-tailed behavior, while differing in how these features are introduced into the spatial process. These structural differences give rise to distinct distributional and inferential properties, which are explored.

2.1. The Nested Construction

The first construction extends the univariate skew-normal Tukey-h (SNTH) distribution (Mondal and Genton, 2024) to a spatial setting through a nested transformation. Specifically, a Tukey-h transformation is applied to a skew-Gaussian random field, yielding a non-Gaussian spatial process with flexible marginal behavior. Formally, the field is defined as

$$\eta_N(\mathbf{s}) = \tau_h\big(W(\mathbf{s})\big),$$

where $\tau_h(x) = x\exp(hx^2/2)$ for $h \geq 0$, and $W(\mathbf{s})$ denotes the skew-Gaussian random field introduced by Zhang and El-Shaarawi (2010):

$$W(\mathbf{s}) = \alpha|Z_1(\mathbf{s})| + Z_2(\mathbf{s}).$$

Here, $Z_1(\mathbf{s})$ and $Z_2(\mathbf{s})$ are independent, stationary Gaussian processes with mean zero, unit variance, and correlation functions $C_{\theta_k}(\cdot)$. In this design, the skewness (α) and tail-heaviness (h) parameters are linked through a nonlinear transformation of the skew-Gaussian field.

2.1.1. Marginal Distribution

To better understand the distributional behavior of the proposed model, we first consider the marginal distribution of the underlying process $W(\boldsymbol{s})$. Following Mondal et al. (2023), $W(\boldsymbol{s})$ follows a skew-normal distribution with location 0, scale 1, and skewness parameter α. Its probability density function (pdf) can be written in closed form as

$$f_{W(\boldsymbol{s})}(w) = 2\,\phi(w; 0, 1+\alpha^2)\,\Phi\left(\frac{\alpha w}{\sqrt{1+\alpha^2}}\right), \quad w \in \mathbb{R}, \tag{1}$$

highlighting how the parameter α induces asymmetry in the marginal law. Here, $\phi(w; 0, 1+\alpha^2)$ denotes the probability density function of a normal distribution with mean zero and variance $1+\alpha^2$, and $\Phi(\cdot)$ represents the standard normal cumulative distribution function.

Applying the Tukey-h transformation to $W(\boldsymbol{s})$ yields the Skew-Gaussian Tukey-h (SGTH) random field $\eta(\boldsymbol{s})$. Consequently, the marginal distribution of $\eta(\boldsymbol{s})$ can be characterized by the skew-normal Tukey-h (SNTH) law, parameterized by the skewness parameter α and the tail-thickness parameter h. Specifically, the marginal distribution of $\eta(\boldsymbol{s})$

can be expressed as $\mathcal{SNTH}(\alpha, h)$ with the corresponding probability density function

$$f_{\eta(s)}(u) = 2\,\phi\big(g(u); 0, 1+\alpha^2\big)\,\Phi\left(\frac{\alpha\, g(u)}{\sqrt{1+\alpha^2}}\right)\left(\frac{\exp\left[\frac{1}{2}W_0\big(hu^2\big)\right]}{hu^2 + \exp\big[W_0\big(hu^2\big)\big]}\right), \tag{2}$$

where

$$g(u) = u\exp\Big(-\tfrac{1}{2}W_0(hu^2)\Big),$$

and $W_0(\cdot)$ denotes the principal branch of the Lambert-W function. The transformation $g(u)$ maps the variable u into the skew-normal domain, thereby preserving tractability while extending flexibility. Although the density involves the Lambert-W function, it remains analytically manageable and suitable for both evaluation and simulation.

2.1.2. First- and Second-Order Moments

By construction, $W(\boldsymbol{s})$ follows a skew-normal distribution (Azzalini, 1985) with mean and variance given by:

$$\mathbb{E}[W(\boldsymbol{s})] = \alpha\sqrt{\frac{2}{\pi}}, \qquad \mathrm{Var}[W(\boldsymbol{s})] = 1 + \alpha^2\left(1 - \frac{2}{\pi}\right).$$

Consequently, applying the Tukey-h transformation, the mean and variance of the SGTH field $\eta(\boldsymbol{s}) = \tau_h(W(\boldsymbol{s}))$ are derived as:

$$\mathbb{E}[\eta(\boldsymbol{s})] = \sqrt{\frac{2}{\pi}}\frac{\alpha}{\sqrt{1-h}\,\{1-h(1+\alpha^2)\}}, \quad \text{for } h < \frac{1}{1+\alpha^2},$$

and

$$\mathrm{Var}[\eta(\boldsymbol{s})] = \frac{1+\alpha^2}{(1-2h(1+\alpha^2))^{3/2}} - \frac{2}{\pi}\frac{\alpha^2}{(1-h)\{1-h(1+\alpha^2)\}^2},$$

for $h < \frac{1}{2(1+\alpha^2)}$.

2.1.3. Covariance Function

The covariance structure of the SGTH field extends beyond the marginal properties, capturing the spatial dependence. For two locations $\boldsymbol{s}, \boldsymbol{s}' \in D$ with $d = \|\boldsymbol{s} - \boldsymbol{s}'\|$, the second joint moment is given by:

$$\mathbb{E}[\eta(\boldsymbol{s})\eta(\boldsymbol{s}')] = \mathbb{E}\left[W(\boldsymbol{s})W(\boldsymbol{s}')\exp\left(\frac{h}{2}(W(\boldsymbol{s})^2 + W(\boldsymbol{s}')^2)\right)\right].$$

This expectation involves a nonlinear transformation of the bivariate random vector $(W(\boldsymbol{s}), W(\boldsymbol{s}'))$. The following lemma provides a semi-closed-form expression for this key quantity, reducing it to a two-dimensional integral of an explicit, well-behaved function.

Lemma 1. *Let $U_1 = \alpha|Z_1| + W_1$ and $U_2 = \alpha|Z_2| + W_2$, where $(Z_1, Z_2)^\top$ and $(W_1, W_2)^\top$ are independent bivariate Gaussian vectors with zero means, unit variances, and correlations ρ_1 and ρ_2, respectively. Then, for $h \geq 0$, the expectation*

$$\mathcal{E} = \mathbb{E}\left[U_1U_2\exp\left(\frac{h}{2}U_1^2 + \frac{h}{2}U_2^2\right)\right],$$

admits the representation:

$$\mathcal{E} = \sum_{s_1,s_2\in\{\pm1\}}\int_0^\infty\int_0^\infty F(a,b;\rho_2)\,\phi(s_1a, s_2b; \rho_1)\,da\,db, \tag{3}$$

where $\phi(\cdot,\cdot;\rho_1)$ is the bivariate normal density of (Z_1, Z_2), and for $a, b \geq 0$,

$$F(a,b;\rho_2) = \frac{\partial^2}{\partial t_1 \partial t_2}\left[e^{\frac{h}{2}\boldsymbol{\mu}^\top\boldsymbol{\mu}+\boldsymbol{t}^\top\boldsymbol{\mu}}\, A\left(h,\rho_2;\, h\alpha a + t_1,\, h\alpha b + t_2\right)\right]\Bigg|_{\boldsymbol{t}=\mathbf{0}}. \tag{4}$$

Here, $\boldsymbol{\mu} = (\alpha a, \alpha b)^\top$, $\boldsymbol{t} = (t_1, t_2)^\top$, and $A(h,\rho;b_1,b_2)$ is the closed-form function

$$A(h,\rho;b_1,b_2) = \frac{1}{\sqrt{D(h,\rho)}}\exp\left(\frac{A_0(b_1^2+b_2^2)+2\rho b_1 b_2}{2D(h,\rho)}\right),$$

with $D(h,\rho) = (1-h)^2 - h^2\rho^2$ and $A_0 = 1-h+h\rho^2$, valid for $D(h,\rho) > 0$.

Proof. The proof follows by conditioning on $(|Z_1|, |Z_2|) = (a, b)$ and exploiting the independence between (Z_1, Z_2) and (W_1, W_2). The conditional expectation

$$F(a,b;\rho_2) = \mathbb{E}_W\left[(\alpha a + W_1)(\alpha b + W_2)\exp\left(\frac{h}{2}(\alpha a + W_1)^2 + \frac{h}{2}(\alpha b + W_2)^2\right)\right],$$

is computed by interpreting it as the second mixed derivative of a moment-generating function, evaluated at zero. The result follows by differentiating the function $M(t_1, t_2)$ defined in the main text. The final expression is obtained by integrating $F(a,b;\rho_2)$ against the joint density of $(|Z_1|, |Z_2|)$, which, due to the symmetry of the bivariate normal distribution, is given by summing over the four sign combinations of (s_1, s_2). □

Remark 1 (Computability). The function $F(a,b;\rho_2)$ in (4) can be computed explicitly by applying the product rule for differentiation. This yields an expression of the form $F(a,b;\rho_2) = P(a,b)\cdot A(h,\rho_2; h\alpha a, h\alpha b)$, where $P(a,b)$ is a polynomial in a and b whose coefficients are functions of h, α, ρ_2. Consequently, the double integral in (3) reduces to a sum of integrals of the form $\int_0^\infty\int_0^\infty p(a,b)\exp(Q(a,b))\,da\,db$, where $p(a,b)$ is a polynomial and $Q(a,b)$ is a quadratic form. These integrals are well-behaved and can be evaluated efficiently using Gaussian quadrature or other standard numerical techniques. Thus, Lemma 1 provides a tractable method for calculating the second moment.

Finally, the covariance function of the SGTH field is given by:

$$\mathrm{Cov}\big(\eta(\boldsymbol{s}), \eta(\boldsymbol{s}')\big) = \mathbb{E}[\eta(\boldsymbol{s})\eta(\boldsymbol{s}')] - \mathbb{E}[\eta(\boldsymbol{s})]\,\mathbb{E}[\eta(\boldsymbol{s}')],$$

where $\mathbb{E}[\eta(\boldsymbol{s})]$ is provided in closed form in Subsection 2.1.2, and $\mathbb{E}[\eta(\boldsymbol{s})\eta(\boldsymbol{s}')]$ is computed via the numerically efficient semi-closed-form expression provided in Lemma 1.

This formulation highlights how the Tukey-h transformation nonlinearly inflates both the variance and covariance relative to the base skew-Gaussian field. As $h \to 0$, the covariance function reduces to that of the skew-Gaussian random field of Zhang and El-Shaarawi (2010).

2.2. Additive Structure

The second model adopts an additive structure:

$$\eta_A(\mathbf{s}) = \alpha|Z_1(\mathbf{s})| + \tau_h\big(Z_2(\mathbf{s})\big).$$

Here, the skew component $(\alpha|Z_1|)$ and the heavy-tailed component $(\tau_h(Z_2))$ are separately constructed and then summed, leading to a decoupled parameterization. This additive specification offers enhanced interpretability, as the parameters α and h directly and independently control skewness and tail behavior, respectively.

Deriving a closed-form marginal density for $\eta(\mathbf{s})$ is challenging, as it involves the convolution of two independent, non-standard distributions: a half-normal and a Tukey-transformed normal. The resulting density does not admit a simple closed form and is best expressed as an integral:

$$f_\eta(y) = \int_0^\infty f_{\alpha|Z_1|}(y-u)\, f_{\tau_h(Z_2)}(u)\,du,$$

where $f_{\alpha|Z_1|}$ and $f_{\tau_h(Z_2)}$ are the densities of the skew and heavy-tailed components. The mean, variance, and covariance functions are given by:

$$\mathbb{E}[\eta_A(\mathbf{s})] = \alpha\sqrt{\frac{2}{\pi}},$$

$$\mathrm{Var}(\eta_A(\mathbf{s})) = \alpha^2\left(1-\frac{2}{\pi}\right) + (1-2h)^{-3/2}, \quad \text{for } h < \frac{1}{2},$$

$$\mathrm{Cov}(\eta_A(\mathbf{s}), \eta_A(\mathbf{s}')) = \mathrm{Cov}(\alpha|Z_1(\mathbf{s})|, \alpha|Z_1(\mathbf{s}')|) + \mathrm{Cov}(\tau_h(Z_2(\mathbf{s})), \tau_h(Z_2(\mathbf{s}'))).$$

Using the known covariance of the skew-Gaussian field (Zhang and El-Shaarawi, 2010) and the approximation for the Tukey-h field (Xu and Genton, 2017), we obtain the closed-form approximation:

$$\mathrm{Cov}(\eta_A(\mathbf{s}), \eta_A(\mathbf{s}')) \approx \frac{2\alpha^2}{\pi}\left(\sqrt{1-\rho_1^2} + \rho_1 \arcsin(\rho_1) - 1\right) + \frac{\rho_2}{[1-2h\rho_2^2]^{3/2}},$$

where $\rho_1 = C_{\theta_1}(d)$ and $\rho_2 = C_{\theta_2}(d)$. Since both components arise from valid stochastic processes, their sum defines a valid covariance function.

A major difference between the nested and additive models is how their parameters are constrained. In the nested model, the existence of finite moments (such as variance) depends on both parameters simultaneously. For example, the variance exists only if $h < \frac{1}{2(1+\alpha^2)}$. This means the allowed range for tail-heaviness (h) is tied to the amount of skewness (α). In contrast, the additive model separates these constraints. As shown in Proposition 1, the variance exists as long as $h < 1/2$, regardless of the value of α. This structural decoupling not only simplifies moment conditions but also has important implications for posterior behavior, as illustrated in the simulation study.

3. Bayesian Hierarchical Modeling with SGTH Spatial Random Effects

We consider a Bayesian hierarchical framework for spatially indexed data, in which the latent spatial random effects are modeled using the class of SGTH spatial fields introduced in Section 2. We model spatially indexed data $Y(\mathbf{s})$ observed at locations $\mathbf{s}_1, \ldots, \mathbf{s}_n \in D \subset \mathbb{R}^2$. The baseline formulation is

$$Y(\mathbf{s}) \mid \beta, \eta(\mathbf{s}), \omega^2) \sim \mathrm{N}\big(\mathbf{x}(\mathbf{s})^\top \boldsymbol{\beta} + \sigma\eta(\mathbf{s}), \omega^2\big), \tag{5}$$

where $\mathbf{x}(\mathbf{s}_i)$ is a p-dimensional covariate vector. Under the additive SGTH model, $\eta(\mathbf{s}) = \alpha|Z_1(\mathbf{s})| + \tau_h\big(Z_2(\mathbf{s})\big)$, while under the nested SGTH model, $\eta(\mathbf{s}) = \tau_h\big(\alpha|Z_1(\mathbf{s})| + Z_2(\mathbf{s})\big)$. The Gaussian fields $Z_1(\mathbf{s})$ and $Z_2(\mathbf{s})$ are independent, stationary, and isotropic with exponential correlation

$$C_\theta(d) = \exp\Big(-\frac{d}{\theta}\Big), \qquad d = \|\mathbf{s} - \mathbf{s}'\|.$$

3.1. Prior Specification

We complete the hierarchy of the model by specifying the prior distribution for the vector of the model parameters, i.e. $\boldsymbol{\psi} = (\boldsymbol{\beta}', \omega^2, \alpha, \sigma, \theta, h)'$. The components of the parameter vector were initially assumed to be independent a priori. Then, proper prior distributions were assigned to the parameters. Below, the selection of the priors is explained.

Prior to regression coefficients $\boldsymbol{\beta}$: We simply take the conjugate multivariate normal

$$\pi(\boldsymbol{\beta}) = N_k(\mathbf{m}_\beta, c_\beta \mathbf{I}_k), \tag{6}$$

where the hyperparameter c_β can be chosen to be sufficiently large to ensure the prior distribution is vague.
Prior for nugget effect parameter ω^2: The ω^2 is assigned an inverse gamma prior:

$$\omega^2 \sim \text{Inv-Gamma}(r, s),$$

with small hyperparameters (r, s) yielding a weakly informative prior.
Prior for Scale parameter σ. Following Gelman (2006), we specify a weakly informative uniform prior on the standard deviation:

$$\sigma \sim \text{Uniform}(0, k_\sigma),$$

where the upper bound k_σ can be chosen to be large but finite values so that the resulting uniform distributions are weakly informative (Gelman, 2006).

Prior to α: The skewness parameter is expected to have a rather restricted range in practice. For example, one could have some prior knowledge about the direction of skewness. Hence, we will use a conjugate truncated normal prior for the skewness parameters α as

$$\pi(\alpha) = f_{TN}(\alpha|a, b; m_\alpha, c_\alpha), \tag{7}$$

where $f_{TN}(\alpha|a, b; m_\alpha, c_\alpha)$ denotes the $N(m_\alpha, c_\alpha)$ distribution truncated to the interval (a, b). By this choice, the hyperparameters a and b show our knowledge about the possible values for the skewness parameter. The hyperparameter m_α should be chosen in the interval (a, b) which is an indication of the mode of our priori knowledge. Finally, the value of c_α sets uncertainty on m_α.

Prior to range parameter θ: In general, the prior specification for the range parameter should depend on the chosen correlation function and the scaling of the distance d. In the literature, the prior for the range parameter is typically chosen so that the effective range covers the maximum distance between spatial locations (see, e.g., Zareifard and Khaledi (2021)). Following this approach, and consistent with the specification used by Zareifard et al. (2018), we assign a gamma prior to the range parameter θ:

$$\theta \sim \text{Gamma}(s, r), \tag{8}$$

where the hyperparameters s and r are chosen as in Zareifard and Khaledi (2021).

Prior to Tail–heaviness parameter h: Finally, for the tail parameter h, we adopt a weakly informative uniform prior over a plausible range of values which permits sufficient flexibility in modeling heavy-tailed behavior without imposing strong prior beliefs.

3.2. Posterior Computation

Bayesian inference for the proposed spatial SGTH random effects model is carried out using Markov chain Monte Carlo (MCMC) simulation. Because the Tukey–h transformation renders the latent field non-Gaussian, we employ a data augmentation strategy based on the underlying skew-Gaussian representation. Specifically, we introduce the latent vectors $\mathbf{Z}_1 = (Z_1(\mathbf{s}_1), \ldots, Z_1(\mathbf{s}_n))^\top$ and $\mathbf{Z}_2 = (Z_2(\mathbf{s}_1), \ldots, Z_2(\mathbf{s}_n))^\top$. Now, given the observed data $\mathbf{y} = (y(\mathbf{s}_1), \ldots, y(\mathbf{s}_n))^\top$, the joint posterior distribution of parameters and latent variables is

$$\begin{aligned}\pi(\boldsymbol{\psi}, \mathbf{z}_1, \mathbf{z}_2 \mid \mathbf{y}) \propto & \prod_{i=1}^{n} f_N\left(y(\mathbf{s}_i) \,\middle|\, \mathbf{x}(\mathbf{s}_i)^\top \boldsymbol{\beta} + \sigma\eta(\mathbf{s}_i), \omega^2\right) \\ & \times f_N^n\left(\mathbf{z}_1 \middle| \mathbf{0}, \mathbf{C}\right) f_N^n\left(\mathbf{z}_2 \middle| \mathbf{0}, \mathbf{C}\right) \; \pi(\boldsymbol{\beta})\pi(\omega^2)\pi(\sigma)\pi(\alpha)\pi(\theta)\pi(h),\end{aligned}$$

where $f_N^k(\cdot)$ denotes the k-multivariate normal distribution and $\mathbf{C} = [C_\theta(\mathbf{s}_i, \mathbf{s}_j)]_{n\times n}$. Given this factorization, we construct a block Gibbs sampler that iteratively updates model parameters and latent variables from their full conditional distributions. Posterior simulation is implemented using a hybrid strategy that combines Gibbs updates, Metropolis–

Hastings steps, and discrete-grid sampling, depending on whether the corresponding conditionals admit closed-form expressions. The latent spatial effects are represented by the Gaussian vectors $\mathbf{Z}_k$, $k = 1, 2$, with prior $\mathbf{Z}_k \sim \mathcal{N}_n(\mathbf{0}, \mathbf{C})$. These vectors are updated element-wise within the Gibbs sampler. Partitioning $\mathbf{Z}_k = (Z_{k,i}, \mathbf{Z}_{k,-i})^\top$ and the covariance matrix accordingly, standard Gaussian conditioning yields the exact full conditional

$$Z_{k,i} \mid \mathbf{Z}_{k,-i} \sim \mathcal{N}\Big(\mathbf{c}_{i,-i}\mathbf{C}_{-i,-i}^{-1}\mathbf{Z}_{k,-i},\ c_{ii} - \mathbf{c}_{i,-i}\mathbf{C}_{-i,-i}^{-1}\mathbf{c}_{-i,i}\Big),$$

where $\mathbf{c}_{i,-i}$ denotes the covariance vector between $Z_{k,i}$ and $\mathbf{Z}_{k,-i}$. Direct evaluation of this conditional requires inversion of the $(n-1)\times(n-1)$ matrix $\mathbf{C}_{-i,-i}$ for every coordinate update, resulting in $\mathcal{O}(n^3)$ computational complexity per sweep, which is prohibitive for moderate or large spatial datasets. To improve scalability, we approximate the above conditional using only a local neighborhood. Let $N_i \subset \{1, \dots, n\} \setminus \{i\}$ denote the set of the m nearest neighbors of location $\mathbf{s}_i$. Conditioning only on this subset yields the approximation

$$Z_{k,i} \mid \mathbf{Z}_{k,N_i} \approx \mathcal{N}\Big(b_i^\top \mathbf{Z}_{k,N_i},\ d_i^2\Big),$$

where

$$b_i = \mathbf{C}_{N_i,N_i}^{-1}\mathbf{c}_{N_i,i}, \qquad d_i^2 = c_{ii} - \mathbf{c}_{i,N_i}\mathbf{C}_{N_i,N_i}^{-1}\mathbf{c}_{N_i,i}.$$

This construction leads to sparse local updates with computational cost $\mathcal{O}(m^3)$ per location with $m \ll n$. Following common practice in nearest-neighbor Gaussian process approximations, we set $m = 20$, which has been shown to provide accurate dependence recovery with substantial computational gains Datta et al. (2016). Although this approximation provides a Gaussian prior conditional, the nonlinear Tukey–h transformation,

$$\eta(\mathbf{s}_i) = \alpha|Z_{1,i}| + \sigma T_h(Z_{2,i}),$$

induces a non-Gaussian likelihood and breaks conjugacy. Consequently, the full conditional

$$\pi(Z_{k,i} \mid \mathbf{Z}_{k,N_i}, \mathbf{y}, \boldsymbol{\psi}) \propto f_N\big(y(\mathbf{s}_i) \mid \mathbf{x}(\mathbf{s}_i)^\top \boldsymbol{\beta} + \eta(\mathbf{s}_i),\ \omega^2\big) \times \pi(Z_{k,i} \mid \mathbf{Z}_{k,N_i}),$$

does not admit a closed-form distribution. We therefore evaluate this density on a finely discretized grid around its local prior mean and sample from the normalized probabilities, yielding a stable and tuning-free discrete Gibbs update. The same grid-based strategy is used for the non-conjugate parameters h and α. Closed-form updates are available for a subset of parameters: $\boldsymbol{\beta}$ is sampled from a Gaussian full conditional, σ from a truncated normal distribution, ω^2 from a inverse gamma distribution, and the range parameter θ is updated via a Metropolis–Hastings step. Posterior samples are stored after burn-in and thinning to reduce autocorrelation. The overall sampling scheme is summarized in Algorithm 1.

3.3. Spatial Prediction

A central goal in geostatistical modeling is prediction at unobserved spatial locations. The following predictive procedure is presented for the additive SGTH model. Prediction under the nested construction follows analogous steps with the corresponding latent components. Let $\mathbf{s}_0$ denote a new spatial location at which no response has been observed. Under the proposed hierarchical model, the quantity of interest is the posterior predictive distribution $p\big(y(\mathbf{s}_0) \mid \mathbf{y}\big)$. Because this distribution does not admit a closed-form expression, prediction is performed via Monte Carlo approximation. Specifically, for each posterior draw of the model parameters and latent variables, we simulate the corresponding latent effects and response at $\mathbf{s}_0$, thereby generating samples from the posterior predictive distribution. The complete procedure for obtaining M posterior predictive samples is summarized in Algorithm 2: The resulting Monte Carlo sample $\{y^{(1)}(\mathbf{s}_0), \dots, y^{(M)}(\mathbf{s}_0)\}$ approximates the posterior predictive distribution. For point prediction, we summarize this distribution using either the posterior predictive mean or the posterior predictive median:

$$\widehat{Y}_{\text{mean}}(\mathbf{s}_0) = \frac{1}{M}\sum_{m=1}^{M} y^{(m)}(\mathbf{s}_0), \qquad \widehat{Y}_{\text{median}}(\mathbf{s}_0) = \text{median}\{y^{(1)}(\mathbf{s}_0), \dots, y^{(M)}(\mathbf{s}_0)\}.$$

Algorithm 1 Block Gibbs sampler for the SGTH spatial model

Initialize $(\boldsymbol{\beta}, \sigma, \omega^2, \theta, \alpha, h, \mathbf{Z}_1, \mathbf{Z}_2)$
for $t = 1, \ldots, T$ **do** ▷ T: total MCMC iterations
  for $k = 1, 2$ **do**
    for $i = 1, \ldots, n$ **do**
      determine neighbor set N_i
      compute local Gaussian prior (b_i, d_i^2)
      discretize a grid around $b_i^\top \mathbf{Z}_{k,N_i}$
      evaluate $\pi(Z_{k,i} \mid \cdot)$ on the grid
      sample $Z_{k,i}$ from normalized discrete probabilities
  sample h via grid-based update
  sample α via grid-based update
  sample $\boldsymbol{\beta}$ from Gaussian full conditional
  sample σ from truncated normal
  sample ω^2 from inverse gamma
  update θ via Metropolis–Hastings
  store samples after burn-in and thinning

The posterior predictive variance is given by

$$\widehat{\mathrm{Var}}\big(Y(\mathbf{s}_0) \mid \mathbf{y}\big) = \frac{1}{M} \sum_{m=1}^{M} \big(y^{(m)}(\mathbf{s}_0) - \widehat{Y}_{\mathrm{mean}}(\mathbf{s}_0)\big)^2.$$

In the presence of skewness or heavy tails, the posterior predictive median provides a more robust point summary than the mean. For this reason, we report median-based predictions in the real-data application (Section 5), while retaining the variance as a measure of predictive uncertainty.

4. Simulation Study

This section investigates the finite-sample behavior and inferential stability of the two SGTH spatial field constructions, with particular emphasis on the identifiability and posterior behavior of the skewness parameter α and the tail parameter h.

4.1. Simulation Design

We consider a controlled simulation study under fixed and known values of the model parameters, focusing on sensitivity to the tail-heaviness parameter h. Specifically, two values of h are examined: $h \in \{0.2,\ 0.3,\}$. For each value of h, independent datasets are generated under both the baseline (nested) SGTH spatial model and the additive SGTH spatial model. The data-generating process follows the hierarchical structure described in Section 2. For each simulated dataset, observations are generated at $n = 200$ fixed spatial locations randomly sampled from $[0, 3]^2$ according to

$$Y(\mathbf{s}) = \mathbf{x}(\mathbf{s})^\top \boldsymbol{\beta} + \sigma\, \eta(\mathbf{s}) + \varepsilon(\mathbf{s}), \qquad \varepsilon(\mathbf{s}) \sim \mathrm{N}(0, \omega^2),$$

where $\eta(\mathbf{s})$ is drawn from either the nested or additive SGTH spatial field. All parameters other than h are held fixed across simulation scenarios and were set as follows:

$$\beta_0 = 2, \quad \sigma = 1, \quad \alpha = 2, \quad \omega^2 = 0.1, \quad \theta = 0.4.$$

4.2. Bayesian Estimation

For each simulated dataset, Bayesian inference is performed using the MCMC algorithms described in Section 3. All computations were carried out using package R. For each model, four independent MCMC chains of 300,000 iterations were run. For inference, the last 200,000 iterations of each chain were retained, and thinning with a lag of 5

Algorithm 2 Posterior predictive sampling at a new location $\mathbf{s}_0$

Require: posterior draws $\{(\boldsymbol{\psi}^{(m)}, \mathbf{Z}_1^{(m)}, \mathbf{Z}_2^{(m)})\}_{m=1}^{M}$

1: **for** $m = 1, \dots, M$ **do**

2: compute cross-covariance vector

$$\mathbf{c}_0 = \big(C_\theta(\mathbf{s}_0, \mathbf{s}_1), \dots, C_\theta(\mathbf{s}_0, \mathbf{s}_n)\big)^\top$$

3: **for** $k = 1, 2$ **do**

4: sample latent effect

$$Z_k^{(m)}(\mathbf{s}_0) \sim \mathcal{N}\Big(\mathbf{c}_0^\top \mathbf{C}^{-1} \mathbf{Z}_k^{(m)},\ 1 - \mathbf{c}_0^\top \mathbf{C}^{-1} \mathbf{c}_0\Big)$$

5: compute transformed effect

$$\eta^{(m)}(\mathbf{s}_0) = \alpha^{(m)} |Z_1^{(m)}(\mathbf{s}_0)| + \sigma^{(m)} T_{h^{(m)}}\big(Z_2^{(m)}(\mathbf{s}_0)\big)$$

6: compute conditional mean

$$\mu^{(m)}(\mathbf{s}_0) = \mathbf{x}(\mathbf{s}_0)^\top \boldsymbol{\beta}^{(m)} + \sigma^{(m)} \eta^{(m)}(\mathbf{s}_0)$$

7: draw posterior predictive sample

$$y^{(m)}(\mathbf{s}_0) \sim \mathcal{N}\big(\mu^{(m)}(\mathbf{s}_0),\ \omega^2(m)\big)$$

8: **return** $\{y^{(m)}(\mathbf{s}_0)\}_{m=1}^{M}$

was applied, yielding 40,000 effectively uncorrelated posterior samples per chain. The R codes for the simulation study are available at `https://github.com/zareifard/Additive-SGTH.git`. To assess sensitivity to initialization, we considered four distinct starting values for the skewness and tail parameters,

$$(\alpha^{(0)}, h^{(0)}) \in \{(0.5, 0),\ (0.5, 0.1),\ (1, 0),\ (1, 0.1)\},$$

while all remaining parameters were initialized at their true data-generating values.

Trace plots provided in Appendix A illustrate the MCMC trajectories for h and α across all scenarios. The additive specification demonstrates rapid exploration of the posterior support and consistently stabilizes around the true data-generating values, regardless of initialization. In contrast, the nested model exhibits significant identifiability challenges; it often converges to regions far from the true parameter values and fails to recover the ground truth even after long iterations. This suggests that the nested construction may suffer from a multimodal or poorly-behaved posterior surface, whereas the additive model ensures reliable parameter recovery and superior computational tractability.

To further investigate parameter identifiability of the additive model, we examine the posterior distributions of h and α under four different starting values. Figures 1 and 2 contrast the posterior densities obtained under the additive SGTH model. The posterior mass for both h and α is well centered around the true parameter values.

Figure 1: Posterior density estimates of the parameters h and α obtained under the additive SGTH model using four distinct starting values. The true value is $h = 0.2$.

Figure 2: Posterior density estimates of the parameters h and α obtained under the additive SGTH model using four distinct starting values. The true value is $h = 0.3$.

The results demonstrated that the additive SGTH model consistently converges to the true parameter values, irre-

Table 1
Posterior summaries under the additive SGTH model for different true values of h

Parameter	True value	1st Qu	Median	Mean	3rd Qu	SD	$\hat{R}$
β	2	1.82	1.96	1.97	2.12	0.23	1.00
σ	1	0.48	0.60	0.62	0.74	0.19	1.00
α	2	2.08	2.30	2.25	2.47	0.33	1.00
h	**0.2**	0.15	0.23	0.23	0.32	0.11	1.00
ω^2	0.1	0.04	0.12	0.17	0.25	0.17	1.00
θ	0.4	0.41	0.50	0.53	0.63	0.16	1.00
β	2	1.77	1.94	1.98	2.13	0.31	1.00
σ	1	0.56	0.70	0.72	0.86	0.21	1.01
α	2	1.81	2.08	1.99	2.29	0.45	1.01
h	**0.3**	0.25	0.32	0.32	0.39	0.09	1.00
ω^2	0.1	0.04	0.15	0.23	0.35	0.24	1.00
θ	0.4	0.39	0.48	0.47	0.62	0.18	1.00

spective of the chosen initial values. A comprehensive summary of the posterior estimates for all parameters, based on these two specified values for the tail parameter h, is presented in Table 1. The findings clearly show that the estimates for all parameters are in close agreement with their true values. To formally assess convergence, we employed the Gelman and Rubin convergence diagnostic (Gelman and Rubin, 1992), calculating the potential scale reduction factor ($\hat{R}$). The resulting $\hat{R}$ values for all parameters are provided in the last column of Table 1. For every parameter under study, these $\hat{R}$ values were close to 1 (all below 1.05), indicating excellent chain mixing and satisfactory convergence to the stationary distribution.

A comprehensive summary of the posterior estimates for all parameters, based on these two specified values for the tail parameter h, is presented in Table 1. The findings clearly show that the estimates for all parameters are in close agreement with their true values. To formally assess convergence, we employed the Gelman and Rubin convergence diagnostic (Gelman and Rubin, 1992), calculating the potential scale reduction factor ($\hat{R}$). For all parameters under study, the $\hat{R}$ values were close to 1 (all below 1.05), indicating excellent chain mixing and satisfactory convergence to the stationary distribution.

These findings highlight the practical advantages of the additive construction for Bayesian spatial inference and motivate its exclusive use in the subsequent real-data application.

5. Spatial rainfall prediction in Fars Province of Iran

This section presents an application of the proposed additive SGTH spatial model to annual rainfall data from Fars Province, Iran. Rainfall is a key climatic variable in agricultural planning and water resource management, particularly in regions that are vulnerable to climate variability and change. Fars Province is one of the major agricultural hubs of Iran and plays a critical role in national food security. In recent decades, Iran has experienced substantial climatic fluctuations, including increased variability in precipitation patterns, making accurate spatial modeling and prediction of rainfall increasingly important.

The dataset consists of annual rainfall amounts (in centimeters) recorded at $n = 100$ meteorological stations across Fars Province during the year 2023. Fars Province is located between latitudes $27°3'$ and $31°42'$ north and longitudes $50°30'$ and $55°36'$ east (Figure 3a). The province exhibits considerable topographic heterogeneity, with substantial variation in elevation (Figure 3b), which gives rise to diverse climatic regimes. According to the modified De Martonne classification (Mahbod *et al.*, 2019), these regimes include temperate semi-arid, cold semi-arid, temperate desert arid, cold desert arid, warm desert arid, Mediterranean temperate, and warm semi-arid climates. This pronounced climatic and geographic diversity makes Fars Province an informative testbed for evaluating flexible spatial models.

The spatial distribution of the monitoring stations is shown in Figure 4. For an exploratory data analysis, the histogram of data and the empirical semivariogram of detrended data are plotted in Figure 5. The histogram reveals a markedly right-skewed distribution with apparent heavy-tailed behavior. Such features are commonly observed in rainfall data and motivate the use of non-Gaussian spatial models capable of jointly accommodating skewness and tail

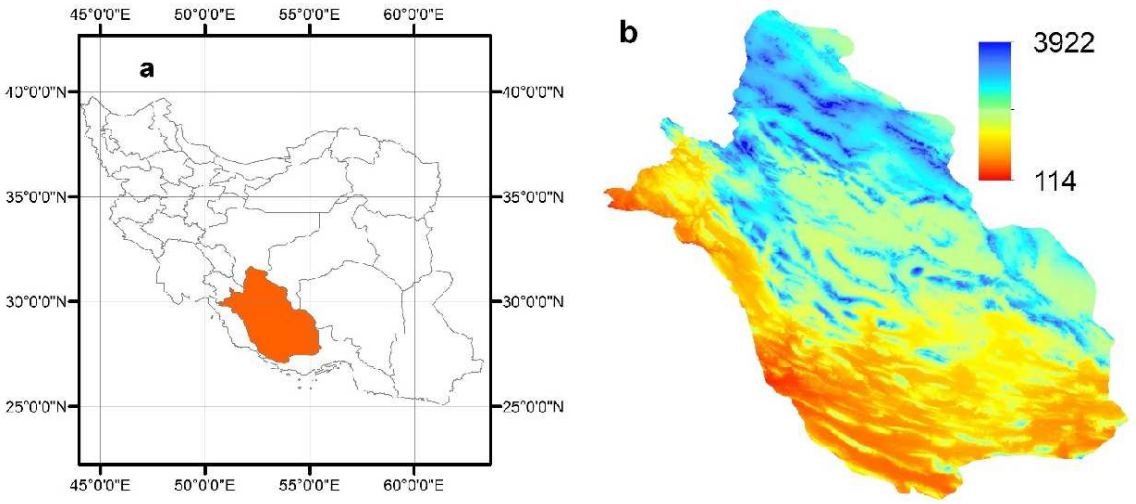


Figure 3: (a) Geographic location of Fars Province in the I.R. Iran; (b) Elevation map of Fars Province.

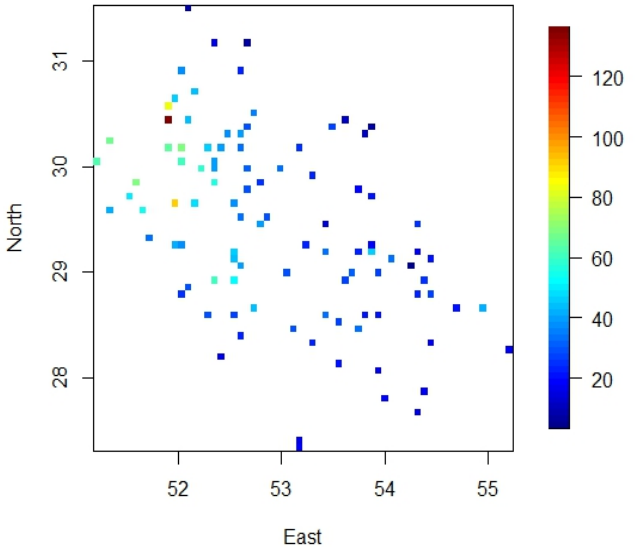


Figure 4: Sampling locations of the rainfall data.

heaviness. Furthermore, the empirical semivariogram of the detrended residuals indicates clear evidence of spatial dependence. To remove large-scale topographic effects, rainfall measurements were first regressed on elevation, and the fitted trend was subtracted from the observations. The proposed SGTH spatial models were subsequently applied to the resulting detrended residuals. Consequently, a constant mean specification ($k = 1$) was adopted, with inference focusing on residual spatial dependence. Bayesian inference is carried out using the additive SGTH spatial random effects model described in Section 3.

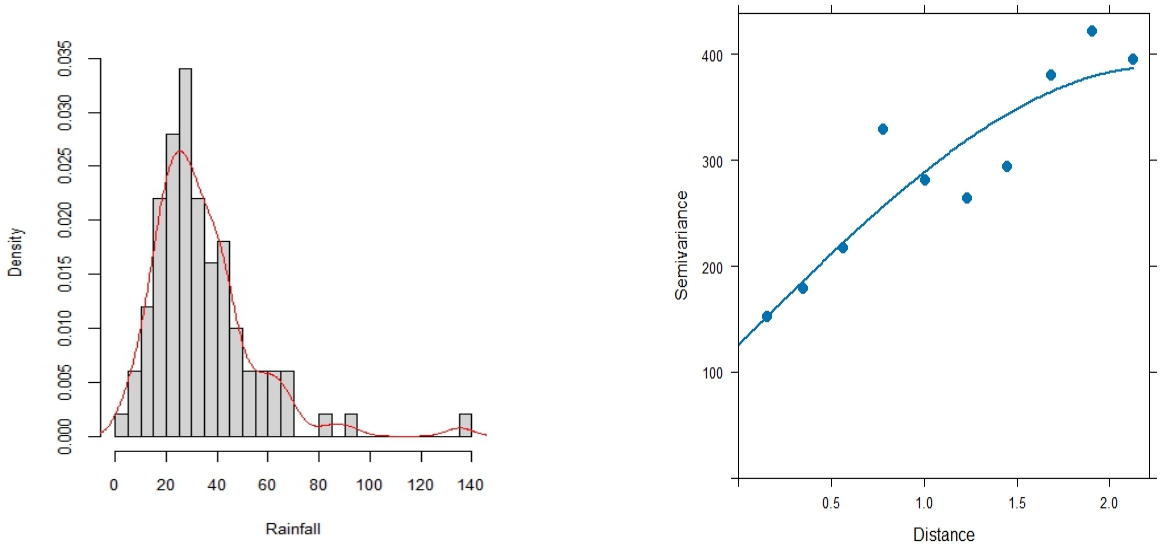


Figure 5: The histogram of data and the empirical semivariogram of detrended data.

For the tail parameter h, we assign a uniform prior on $(0, 3)$. This relatively diffuse prior is chosen to allow for a wide range of tail behaviors, including strongly heavy-tailed regimes. Although the marginal Tukey-h distribution admits finite variance only for $h < 0.5$, our hierarchical formulation does not require finite second moments of the latent transformation. Allowing h to exceed 0.5 enables the model to capture extreme environmental variability when supported by the data.

All computations are performed in the `R` environment. Four independent MCMC chains are run, each consisting of 200,000 iterations. The first 100,000 iterations of each chain are discarded as burn-in, and thinning with a lag of 5 was applied, yielding 20,000 effectively uncorrelated posterior samples. Convergence is assessed using the Gelman–Rubin diagnostic (all $\hat{R} < 1.05$) together with visual inspection of trace plots. We note that posterior computation remains stable and well-behaved despite the implied infinite marginal variance.

Parameter estimates under the additive SGTH spatial random effects model, reported in Table 2, provide clear evidence of spatial dependence as well as significant skewness and heavy-tailed behavior in the rainfall data. The posterior mean of $h = 1.078$ (95% CI: 0.72, 1.37) suggests pronounced heavy-tailed behavior, consistent with the presence of extreme rainfall events in the study region. Given the strongly heavy-tailed behavior indicated by h, we report posterior predictive medians rather than means for spatial prediction, as the median provides a more robust summary in the presence of extreme values.

To evaluate predictive performance, $p = 15$ locations are randomly withheld from the dataset. Prediction accuracy is assessed using the mean squared prediction error (MSPE), defined as

$$MSPE = \frac{1}{p}\sum_{i=1}^{p}\left(y_{0_i} - \hat{y}_{0_i}\right)^2, \tag{9}$$

where y_{0_i} denotes the observed rainfall at location $\mathbf{s}_{0_i}$ and $\hat{y}_{0_i}$ is the corresponding posterior predictive median. Smaller values of MSPE indicate superior predictive performance. Figure 6 displays boxplots of the absolute differences between the observed and predicted values at the 15 withheld locations under the Gaussian model, Gaussian–log-Gaussian model (GLG) of Palacios and Steel (2006), skew-Gaussian model (SG) of Zhang and El-Shaarawi (2010), and additive SGTH model. In this figure, the corresponding MSPE values are shown above each model's boxplot. The superiority of the additive SGTH model, as evidenced by the lower MSPE, highlights the importance of accounting for both skewness and heavy-tails simultaneously in Fars Province, where extreme topographic variations lead to complex precipitation patterns.

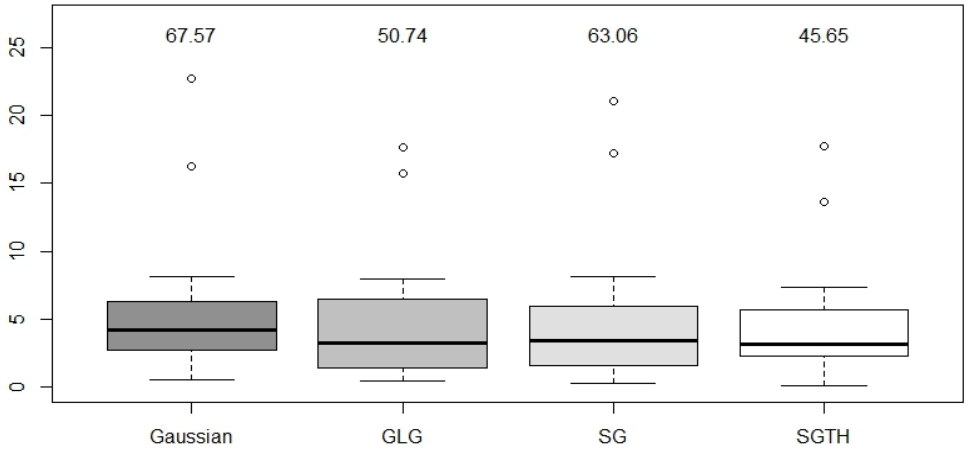


Figure 6: Boxplots of the absolute differences between observed and predicted values at 15 withheld locations for the Gaussian, GLG, SG, and SGTH models. The corresponding MSPE values are displayed above each boxplot.

Table 2
Posterior summaries under the additive SGTH model.

Parameter	1st Qu	Median	Mean	3rd Qu	SD
β	13.00	15.98	16.59	19.59	4.33
σ	11.47	14.70	15.02	18.35	5.14
α	4.910	8.365	7.910	11.160	3.83
h	0.720	1.030	1.078	1.37	0.45
ω^2	11.60	18.51	19.05	25.87	7.17
θ	2.78	3.68	3.53	4.39	1.01

Finally, Figure 7 displays the contour maps of the posterior predictive median rainfall surface (left panel) and the corresponding posterior predictive standard deviation (right panel). The resulting spatial patterns align well with the known climatic and topographic features of Fars Province, highlighting the practical utility of the proposed model for agricultural planning and water resource management.

6. Discussion and Conclusions

This paper introduced a flexible class of skew-Gaussian Tukey-h (SGTH) spatial random fields for modeling spatial data exhibiting joint skewness and heavy-tailed behavior. Motivated by the limitations of standard skew-Gaussian models in capturing extreme events, we proposed two complementary constructions: the nested and additive formulations.

From a theoretical perspective, the nested SGTH construction extends the skew-normal Tukey-h distribution to the spatial domain, offering analytically tractable marginal moments and covariance structures. While these properties serve as a useful methodological benchmark, our simulation results reveal that the nested construction faces significant identifiability challenges. Specifically, the MCMC chains often converge to biased regions far from the true data-generating values, limiting its reliability for parameter recovery.

In contrast, the additive SGTH model, which decouples the mechanisms governing asymmetry and tail behavior, demonstrated robust and consistent inferential performance. Simulation studies confirmed that the posterior distribu-

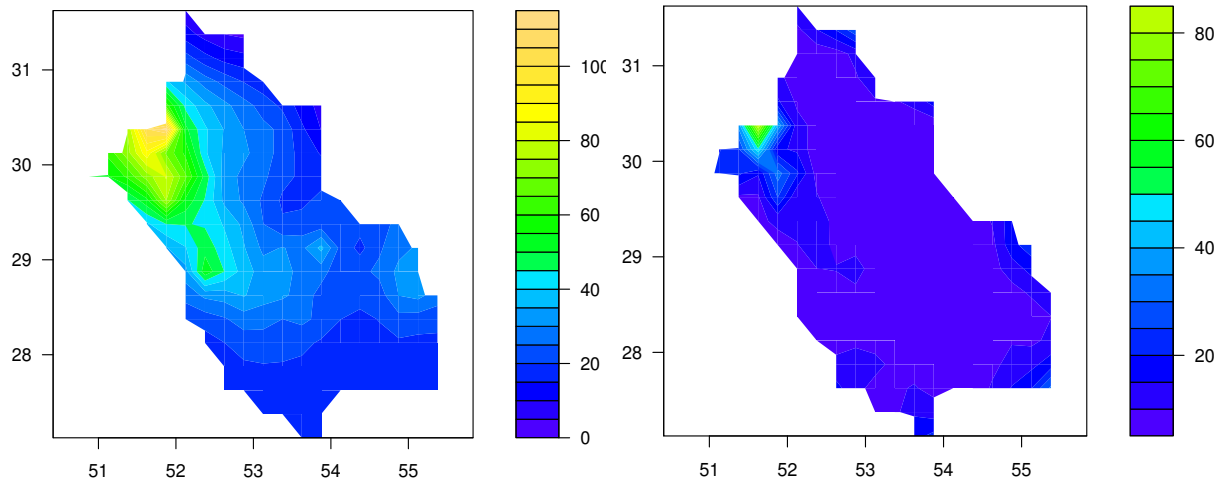


Figure 7: Contour maps of the posterior predictive median rainfall surface (left) and the corresponding posterior predictive standard deviation (right).

tions for both skewness and tail parameters are well-centered around their true values. These findings suggest that the additive construction provides a more stable and practically viable framework for Bayesian modeling of complex non-Gaussian spatial processes.

The practical utility of the additive SGTH model was demonstrated through an application to annual rainfall data in Fars Province, Iran. Our model outperformed Gaussian, log-Gaussian, and skew-Gaussian alternatives in terms of predictive accuracy (MSPE). The results highlight the model's ability to capture the pronounced climatic heterogeneity of the region, providing a powerful tool for agricultural planning and water resource management.

Future research could extend this framework in several directions. Adapting the additive SGTH structure to areal data via conditional autoregressive (CAR) or Gaussian Markov random field (GMRF) models would be highly valuable for regional-level analysis. Furthermore, developing spatio-temporal versions of the SGTH process would allow for modeling the evolution of extreme environmental events over time, a critical need in climate change impact studies.

Appendix A: Trace Plots

This appendix presents the trace plots of the tail parameter h and skewness parameter α under the additive and nested SGTH models for four different initializations: $(\alpha^{(0)}, h^{(0)}) \in \{(0.5, 0), (1, 0), (0.5, 0.1), (1, 0.1)\}$.

References

Azzalini, A. (1985). A Class of Distributions which Includes the Normal Ones. *Scandinavian Journal of Statistics*, **12**, 171–178.

Azzalini, A., and Capitanio, A. (2014). *The Skew-Normal and Related Families*. Cambridge University Press.

Bevilacqua, M., Caamaño-Carrillo, C., Arellano-Valle, R. B., and Morales-Oñate, V. (2021). Non-Gaussian geostatistical modeling using (skew) t processes. *Scandinavian Journal of Statistics*, **48(1)**, 212-245.

Datta, A., Banerjee, S., Finley, A. O., and Gelfand, A. E. (2016). Hierarchical nearest-neighbor Gaussian process models for large geostatistical datasets. *Journal of the American Statistical Association*, **111**, 800-812.

Gelman, A. (2006). Prior distributions for variance parameters in hierarchical models. *Bayesian Analysis*, **1**, 515–533.

Gelman, A., and Rubin, D. B. (1992). Inference From Iterative Simulation Using Multiple Sequences. *Statistical Science*, **7**(4), 457–472.

Mahbod, M., Shirvani, A., and Veronesi, F., 2019. A comparative analysis of the precipitation extremes obtained from tropical rainfall-measuring mission satellite and rain gauges datasets over a semiarid region. *Int. J. Climatol*, 39, 495-515.

Mondal, S., Arellano-Valle, R. B., and Genton, M. G. (2024). A multivariate modified skew-normal distribution. *Statistical Papers*, **65(2)**, 511–555.

Mondal, S., and Genton, M. G. (2024). A Multivariate Skew-Normal-Tukey-h Distribution. *Journal of Multivariate Analysis*, **200**, 105260. Available online 28 November 2023, doi:10.1016/j.jmva.2023.105260.

Palacios, M. B., and Steel, M. F. J. (2006). Non-Gaussian Bayesian Geostatistical Modeling. *Journal of the American Statistical Association*, **101**(474), 604–618.

Schliep, E. M. and Hoeting, J. A. (2013). Multilevel Latent Gaussian Process Model for Mixed Discrete and Continuous Multivariate Response Data. *Journal of Agricultural, Biological, and Environmental Statistics*, 18(4), 492-513.

Xu, G., and Genton, M. G. (2017). Tukey g-and-h random fields. *Journal of the American Statistical Association*, **112(519)**, 1236-1249.

Zareifard, H., and Khaledi, M. J. (2013). Non-Gaussian Modeling of Spatial Data Using Scale Mixing of a Unified Skew Gaussian Process. *Journal of Multivariate Analysis*, **114**, 16–28.

Zareifard, H., Khaledi, M. J., Rivaz, F., and Vahidi-Asl, M. Q. (2018). Modeling Skewed Spatial Data Using a Convolution of Gaussian and Log-Gaussian Processes. *Bayesian Analysis*, **13**(2), 531–557.

Zareifard, H., Khaledi, M. J. (2021). A heterogeneous Bayesian regression model for skewed spatial data. *Spatial Statistics*, **46**, 100545.

Zhang, H., and El-Shaarawi, A. (2010). On Spatial Skew-Gaussian Processes and Applications. *Environmetrics*, **21**(1), 33–47.

Zhang, Q., Schmidt, A. M., and Chaubey, Y. P. (2024). Modelling Left-Censored Skewed Spatial Processes: The Case of Arsenic Drinking Water Contamination. *Spatial Statistics*, 105816.

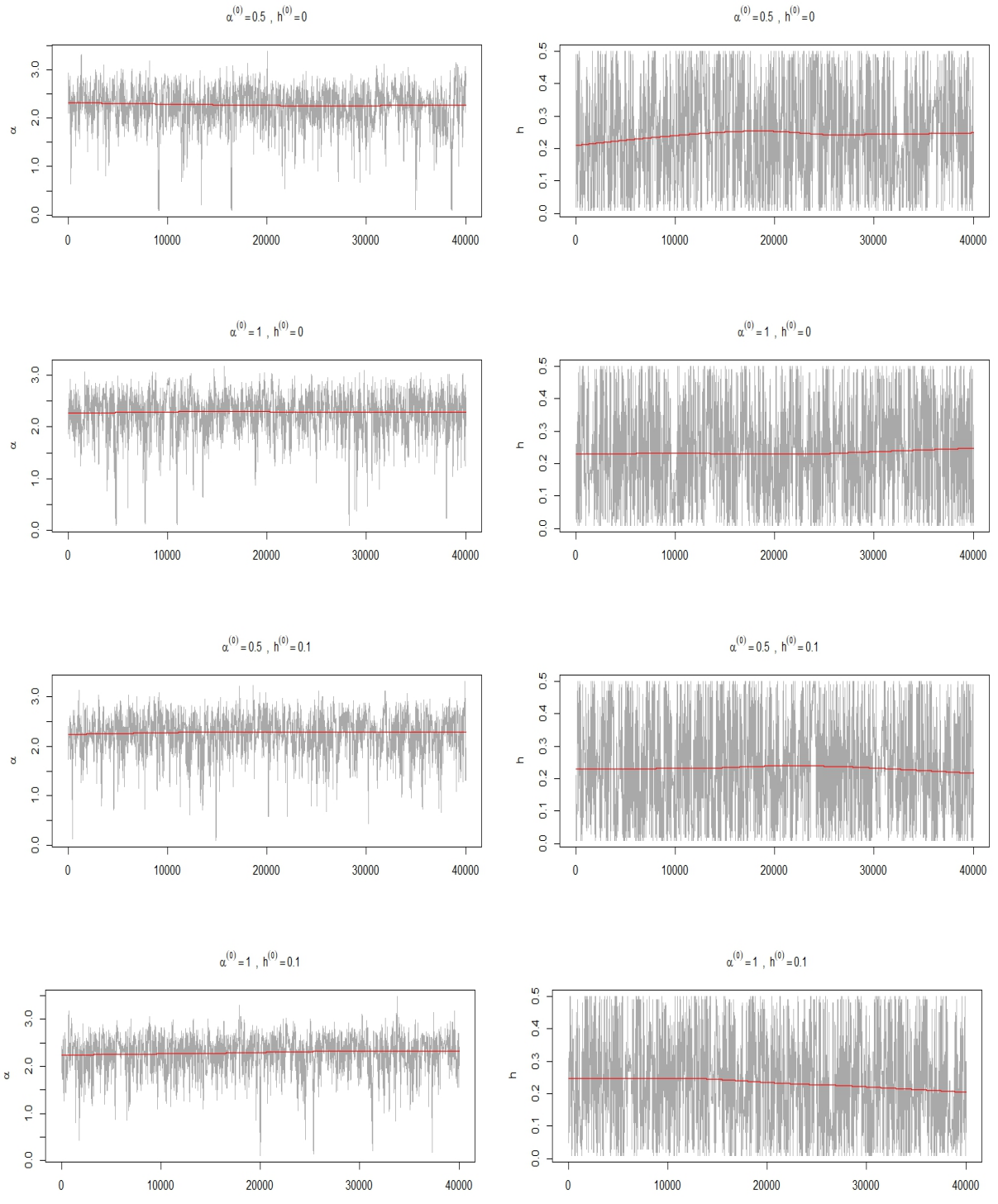


Figure : Trace plots of the tail parameter h and skewness parameter α under the additive SGTH model for four different initializations. The true value is $h = 0.2$. The chains converge to the same stationary distribution, demonstrating the robustness of the posterior inference to initialization.

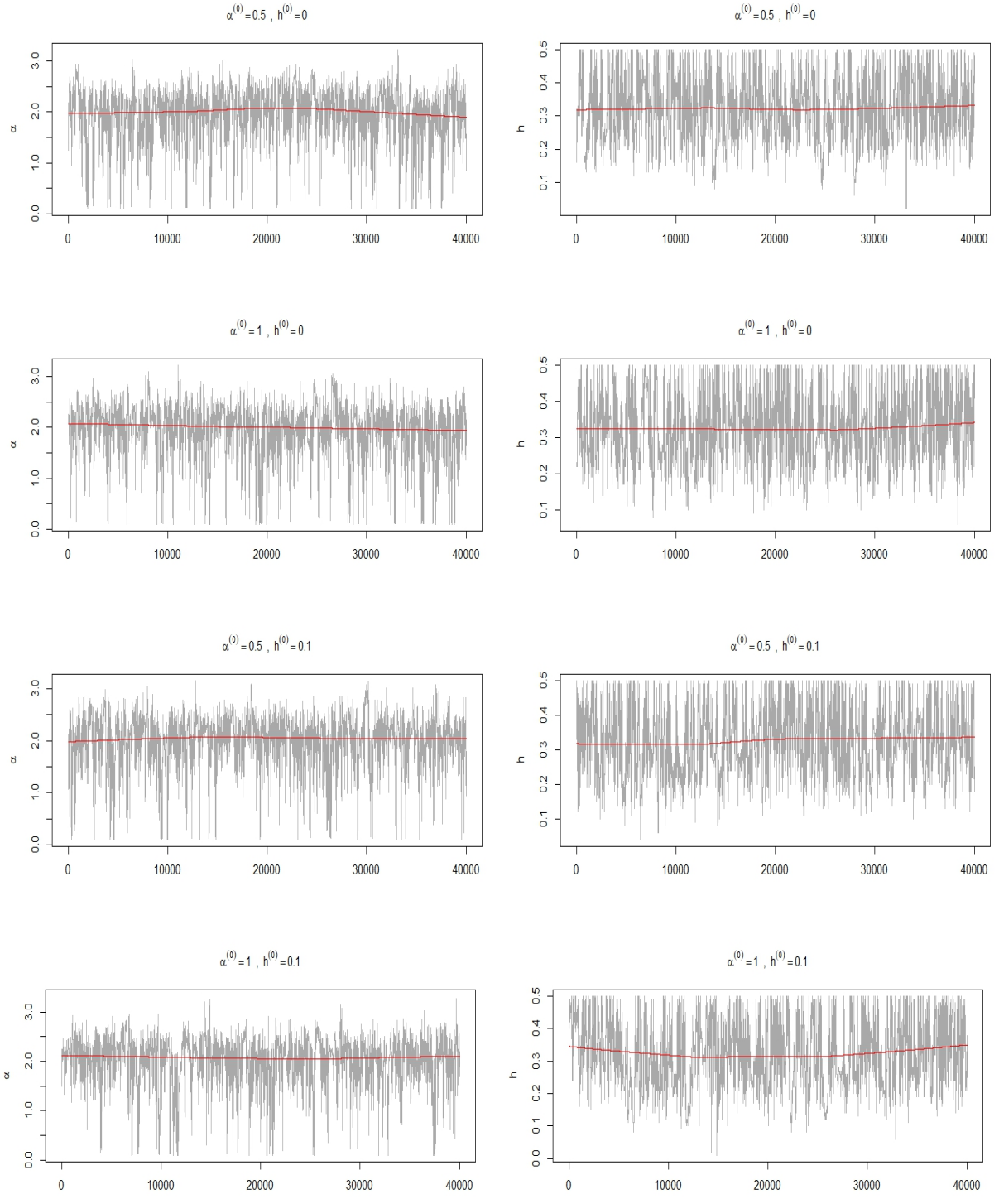


Figure : Trace plots of the tail parameter h and skewness parameter α under the additive SGTH model for four different initializations. The true value is $h = 0.3$. The chains converge to the same stationary distribution, demonstrating the robustness of the posterior inference to initialization.

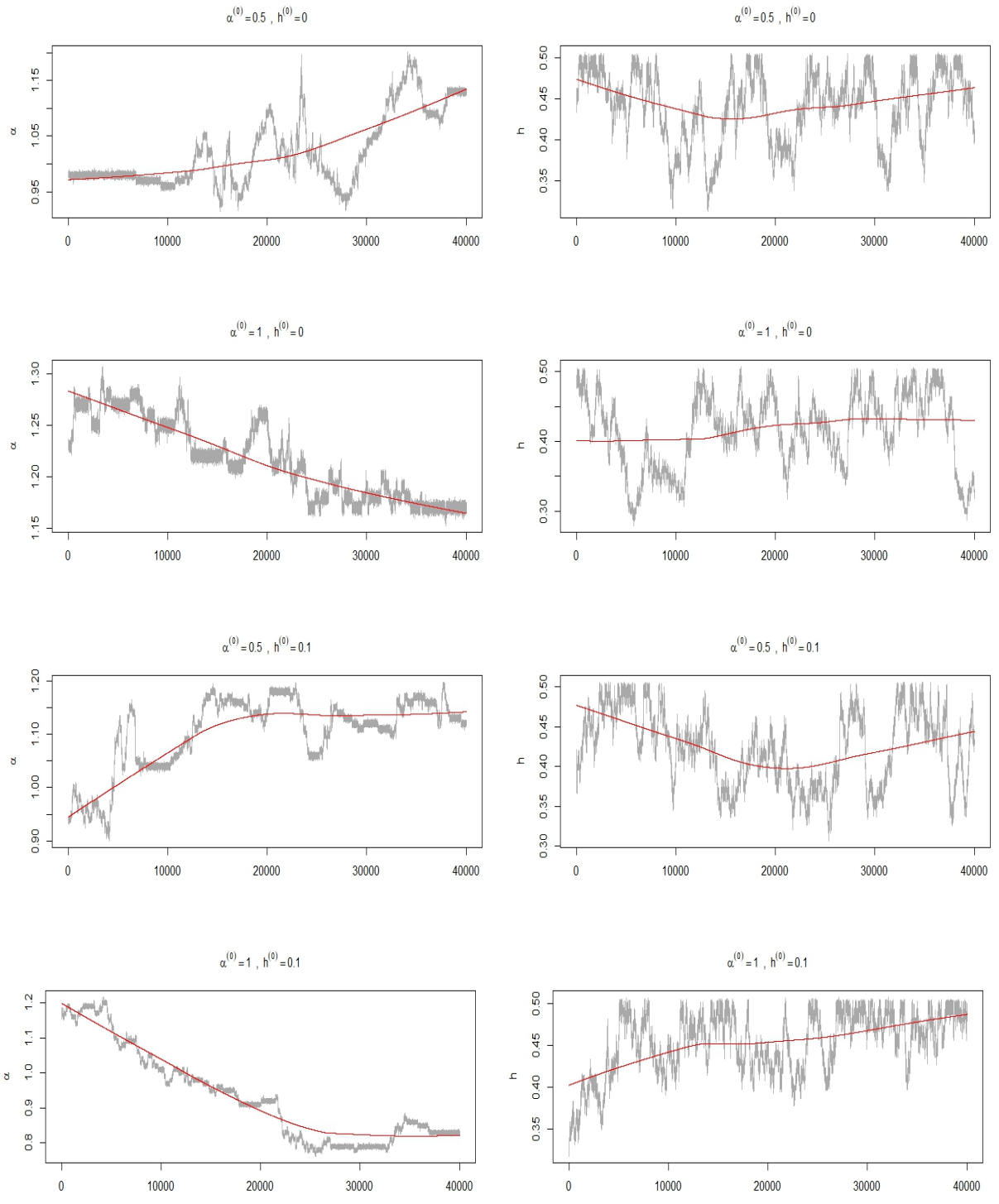


Figure : Trace plots of the tail parameter h and skewness parameter α under the nested SGTH model for four different initializations. The true value is $h = 0.2$.

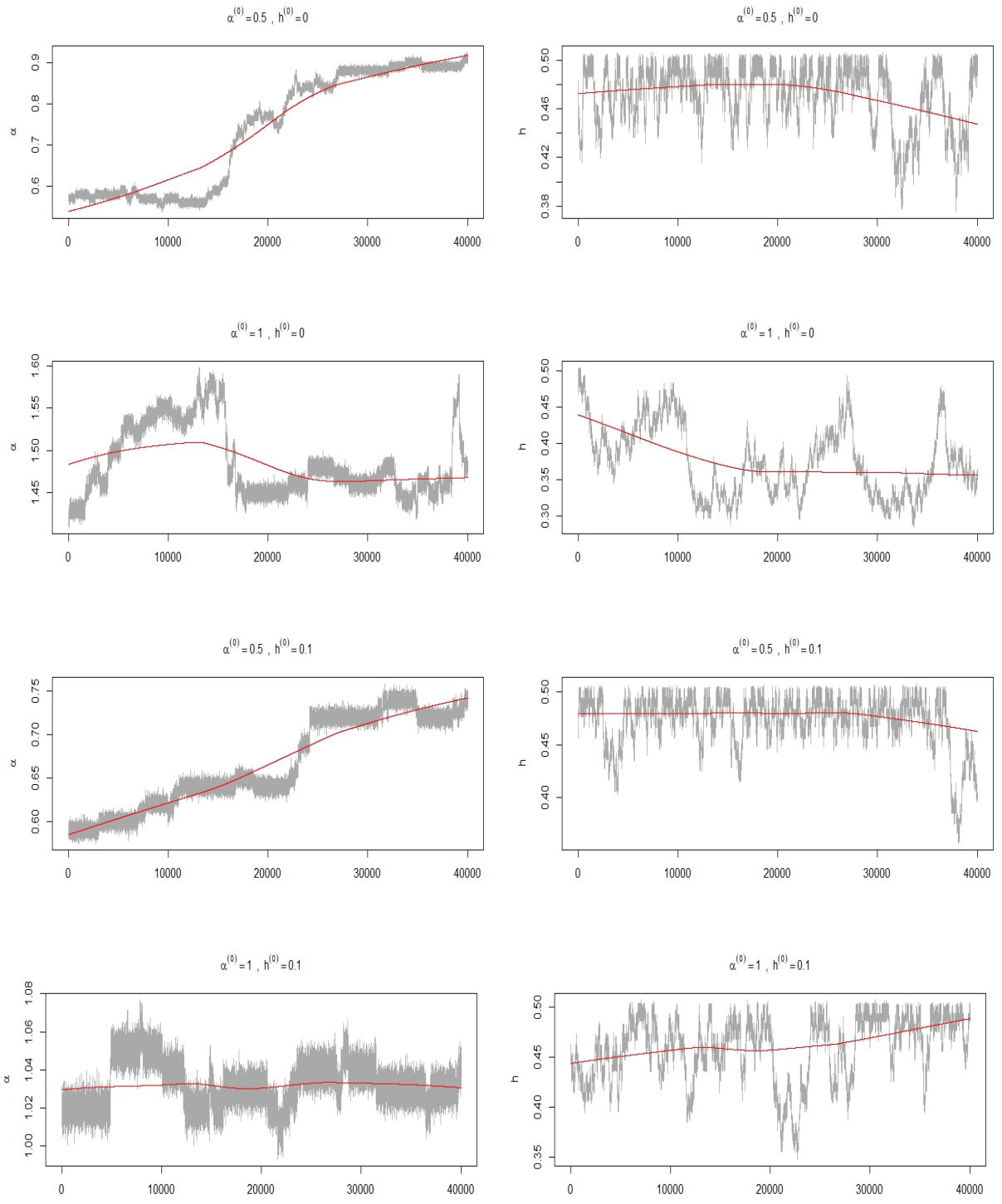


Figure : Trace plots of the tail parameter h and skewness parameter α under the nested SGTH model for four different initializations. The true value is $h = 0.3$.